A water tank muon spectrometer for the characterization of low energy atmospheric muons

Daniela Munteanu, Soilihi Moindjie, Jean-Luc Autran

A water tank muon spectrometer for the characterization of low energy atmospheric muons

D. Munteanu, S. Moindjie, J.L. Autran*

Aix-Marseille Univ, Univ Toulon and CNRS, IM2NP UMR 7334

Faculté des Sciences, Service 142, Avenue Escadrille Normandie Niémen

F-13397 Marseille Cedex 20, France

Abstract

In this work, a water tank muon spectrometer was designed, assembled and operated to measure the energy distribution of low energy atmospheric muon flux induced by cosmic-rays at sea level in the energy range 100-500 MeV. The principle of this experiment is to use water as muon moderator inserted between two coincidence detectors to select the cutoff energy below which muons can no longer be detected. The differential and integral muon spectra are then derived from successive measurements by varying the liquid height within the water tank. The instrument was entirely characterized and modeled in terms of detector efficiency, cutoff energy and counting rate. Experimental data are reported for the energy distribution of muon flux at sea level (43°N of latitude) and finally compared with literature survey.

Keywords: Atmospheric muons, low energy muons, cosmic rays, muon flux, muon spectrometer, sea level muon intensity, differential spectrum, integral spectrum

*Corresponding author. Tel: + 33 413594627, fax: +33 491288531

E-mail address: jean-luc.autran@univ-amu.fr

1. Introduction

Muons are the most abundant energetic charged particles at sea level where they arrive with an average flux of about ≈1 muon per square centimeter and per minute and with an average energy of about 4 GeV [1]. Their characterization provides important information on the physics of primary cosmic rays and on the production mechanisms of atmospheric cascades. An abundant literature exists for muons at ground level and underground but the overwhelming majority of works rather concerns high-energy physics with energy ranges above a few GeV and beyond [2]. Literature surveys on atmospheric muons [2-7] show that there is a clear lack of experimental data typically below a few hundred MeV. In another field of interest, i.e. in radiation effects on modern electronics, the interest for low energy muons is rapidly growing due to the potential role that they can play in failure mechanisms of nanoscale digital integrated circuits [8, 9]. Even if the research effort has so far focused mainly on the errors induced by atmospheric neutrons in electronics [10-14], the effects of muons can no longer be neglected. Indeed, recent investigations demonstrated the importance of these particles in the production of soft errors in the most advanced CMOS technologies [15-18]. The probability of memory upsets was shown to increase near the energy region corresponding to muon stopping in the circuit semiconductor material, indicative of direct ionization effects [16]. The characterization of low energy muon distributions at ground level is thus a challenging issue for the prediction of radiation effects in microelectronics; this corresponds to the initial motivation of the present work.

In this context, we recently developed a muon telescope to measure the cosmic-ray induced atmospheric muon flux at sea level (43°N of latitude) in terms of vertical muon intensity and zenithal angle dependence [19]. However, the energy distribution of the muon flux cannot be measured with the instrument developed in [19]. In the present work, we thus

developed a new instrument, called "water tank muon spectrometer" to precisely measure the energy distribution of atmospheric muons in the range of hundreds of MeV. The principle of this experiment is to use water as muon moderator sandwiched between two detectors in coincidence to select the cutoff energy below which the muons will no longer be detected. It is then possible to determine the energy distribution of muon flux by varying the water height in the water reservoir. This paper details the main characteristics of this instrument including its complete characterization and modeling and reports our first measurements of the muon differential and integral flux in the range 100-500 MeV conducted at sea level in Marseille (43° N of latitude).

2. The water tank muon spectrometer

2.1. Experimental setup

The experimental setup is presented in Figure 1. The muon spectrometer was developed using a dedicated metallic tower structure capable to support heavy load (two metric tons of water in storage tanks) between the two detectors installed at the top and the bottom of the structure. The two detectors are square plastic scintillators (surface of 50x50 cm^2, thickness of 5 cm, housed in 1.5 mm of aluminum plate). The plastic scintillator is made of polyvinyltoluene (PVT) and fabricated by Eljen Technology (EJ-200) [20]. This plastic is highly sensitive to charged particles: its typical stopping power for 1 GeV muons is 2.132 MeV/cm [21]. Each scintillator has a photomultiplier tube (PM) directly integrated in the assembly; the tube is placed in a housing positioned in the bulk material and optically coupled using a high refractive index optical coupling medium at the bottom of the housing (polished surface with an optical quality). The PMs are Hamamatsu model R6427 with 28 mm tube diameter, 25 mm round photocathode and 10-stage photomultiplier. The assembly (PM+scintillator) is mounted in an aluminum housing (thickness 1.5 mm) that ensures a

permanent light sealing. This solution also offers a simplification of detector design by eliminating support hardware to maintain contact between the scintillator material and the PM.

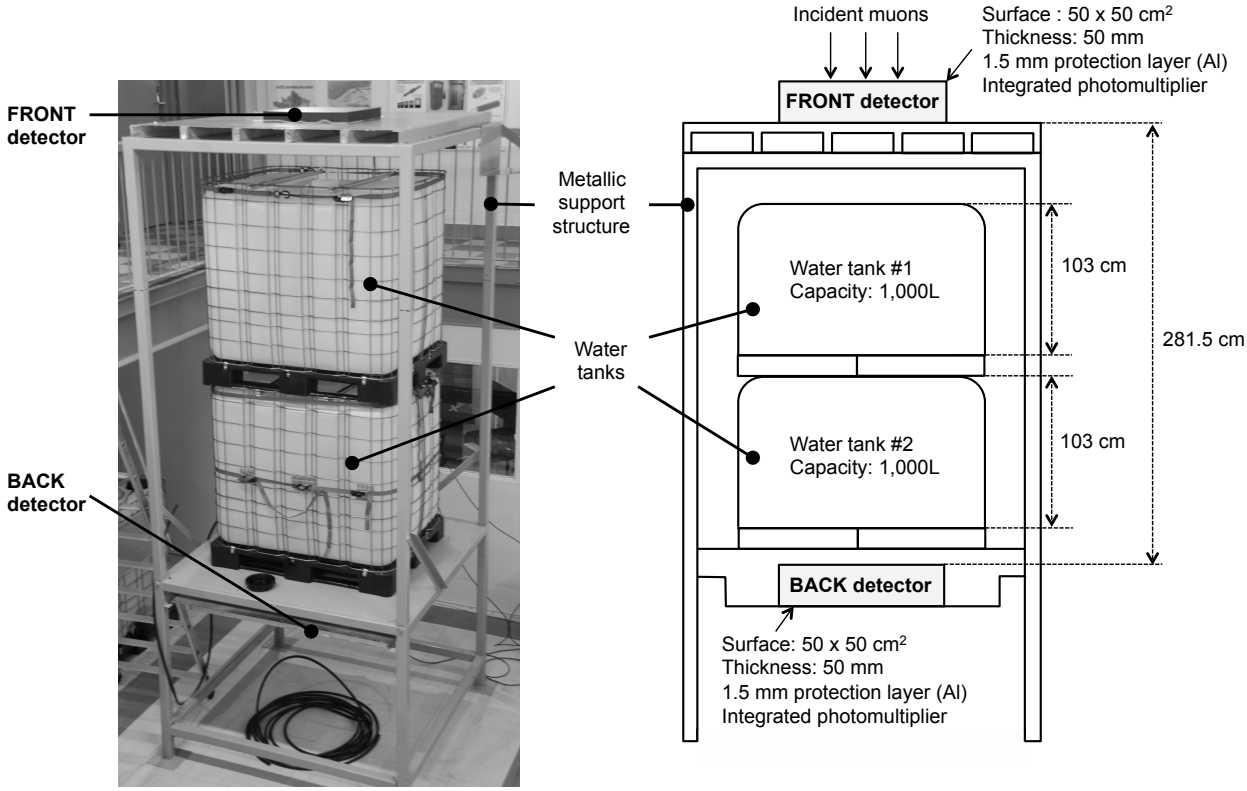

(a) (b)

Figure 1. (a) Front view of the water tank muon spectrometer composed from two square detectors mounted on a metallic support and separated by two water storage tanks made from blow molded high-density polyethylene. The variation of the water level is carried out manually by filling or emptying the tanks with an electrical pump. (b) Schematic representation of the water tank muon spectrometer: the main geometrical parameters and structure configuration are indicated.

The two PMs are connected to the measurement and acquisition chain shown in Figure 2. Photomultipliers convert scintillation light pulses into electrical signals that are then sent to the acquisition chain which trigs the muons traversing the front scintillator and measures, using a coincidence detection procedure in a time window of 10 ns, their time-of-flight

between the front and back detectors separated by a distance of 2.815 m. PM signals as well as time-of-flights converted in voltage pulses using a time-to-amplitude converter (TAC) are digitized using multi-channel analyzers (MCAs based on 16k ADCs). For piloting the experiment, we have developed dedicated Visual Basic software that allows the acquisition of the muon count rate as function of the water level in the water tank. The two polyethylene water tanks have a thickness of about 3 mm except the bottom of the tanks, which has a thickness of 9 mm. The second tank is installed on a stainless steel plate about 2 mm thick. The variation of the water level was carried out manually by filling or emptying the tanks by a step of 100 L, which corresponds to a water height of 9 cm. An additional layer of lead with a thickness of 50 mm was optionally added just below the top detector in order to verify that low energy gamma rays and electrons are satisfactorily rejected in the detector response.

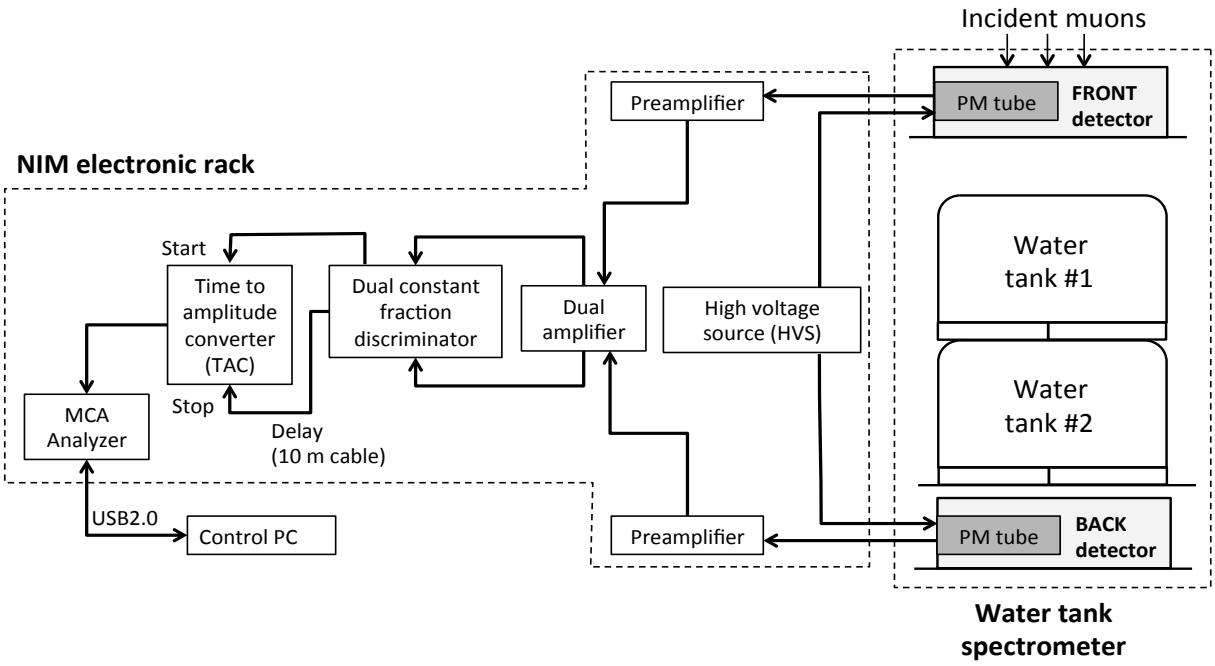

Figure 2. Schematics of the electronics acquisition chain for measuring the time-of-flight of coincidence muons between the two detectors of the spectrometer.

2.2. Spectrometer calibration

In order to optimize the spectrometer operation and to be sure that the spectrometer detects and counts only atmospheric muons, a careful calibration of the instrument has been performed, very similarly to that carried out in [19] for the cosmic ray telescope. The calibration procedure consists in the following three steps:

(i) the detection threshold of the pulses coming out of each PM has been fine-tuned (around 130 mV), which ensures that the low-energy peak (due to the PM noise and the contribution of ambient gamma radiation) is well rejected, the counting rate thus only corresponding to the contribution of the sole charged atmospheric muons (see Fig. 3 in [19] for details) ;

(ii) the nominal value of the supplying voltage (around 1500 V) for each PM has been carefully selected in order to operate in the middle of the plateau of the PM counting rate – voltage characteristics ;

(iii) a calibration of the electronic acquisition chain has been also conducted to determine the MCA channel number versus time proportionality. The MCA was calibrated to a resolution of approximately 160 bins/ns.

Finally, since a detector may sometimes miss (i.e. do not detect) a muon passing through, the efficiency, η, of each detector has been carefully determined using the calibration procedure described in [19]. We found $\eta_F = 99\%$ and $\eta_B = 99\%$ for the front and the back detector, respectively.

2.3. Spectrometer modeling and simulation

2.3.1. Cutoff energy

To be detected by the back detector, muons must cross the instrument with a minimal energy, depending on the level of water in the tanks, called cutoff energy (E_{min}). Extensive

simulations using TRIM (Transport of Ions in Matter) Monte Carlo simulation code [22] have been performed to determine the cutoff energy of the spectrometer for each water level in the tanks. In these simulations we have taken into account the exact 1D stack of materials that the muons pass through from the metal roof of the building to the back detector, including the first floor (air and concrete slab) and the different materials of the spectrometer. Muons have been emulated in TRIM by applying a simple "mass scaling" to protons, as suggested in [23]. We estimate that signal pulses produced by a particle depositing around 2 MeV in the scintillator material of the detector can pass the constant fraction discriminator. Figure 3 and 4 illustrate TRIM simulations used to determine the cutoff energy for a cumulative water level in the tanks of 150 cm. We consider an incident muon arriving in perpendicular incidence on the building roof with an incident energy of 374 MeV. The muon pass through the successive layers from the metallic roof to the back detector and its energy decreases until going to zero in the back detector where it definitely stops and is detected by the coincidence detection procedure. The variation of the muon energy and the energy lost in each layer are shown in Fig. 3 and 4, respectively; the different layers crossed by the muon are also indicated in these figures. Our simulations show that muons with lower incident energies are stopped in the spectrometer layers before reaching the back detector (i.e. they will not be detected by the spectrometer), while muons with higher incident energies are systematically detected by the back detector. This means that the cutoff energy of the spectrometer for a water level of 150 cm is E_{min} = 374 MeV. This value should be slightly higher for oblique tracks. The same procedure was used to determine the cutoff energy of the spectrometer for each level of water in the water tanks. Figure 5 shows the calculated cutoff energy of the spectrometer as a function of the cumulative height of the water level in the two water tanks.

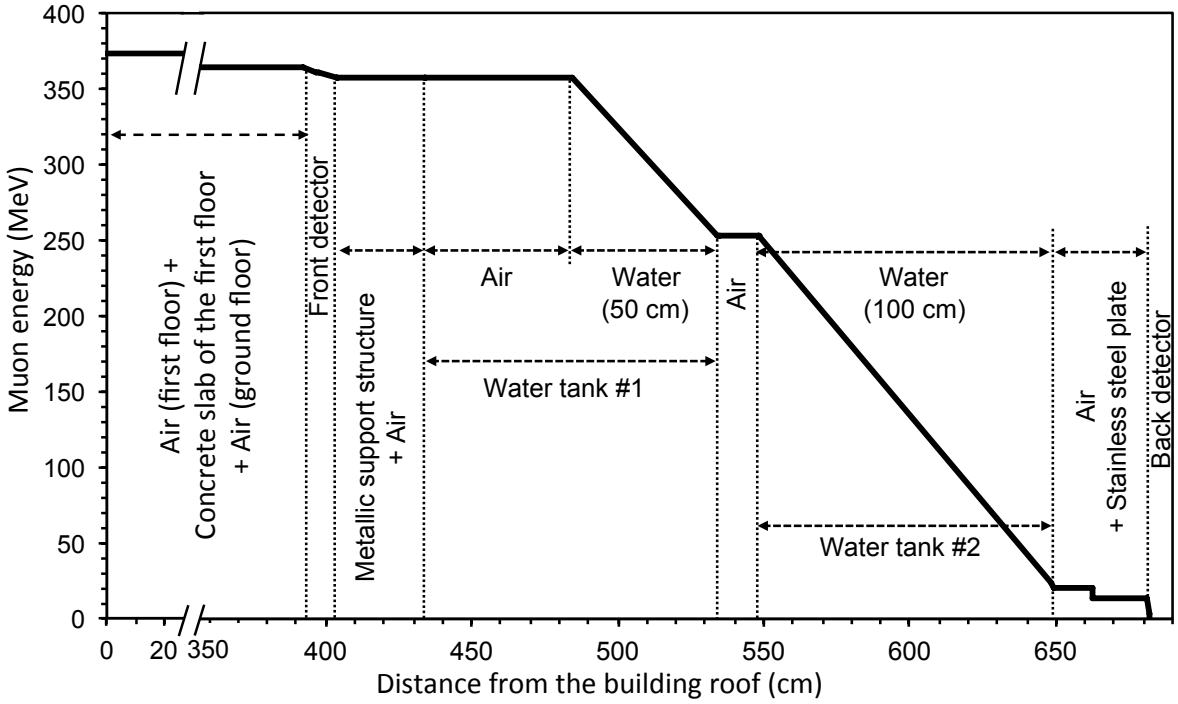

150

151 **Figure 3.** TRIM simulation showing the muon energy variation through the water tank
152 spectrometer for an incident energy of 374 MeV (particle track perpendicular to the detector
153 surfaces). The water height is 50 cm in the first water tank and 100 cm in the second tank.
154 The cutoff energy of the spectrometer for a water level of 150 cm is E_{min} = 374 MeV.

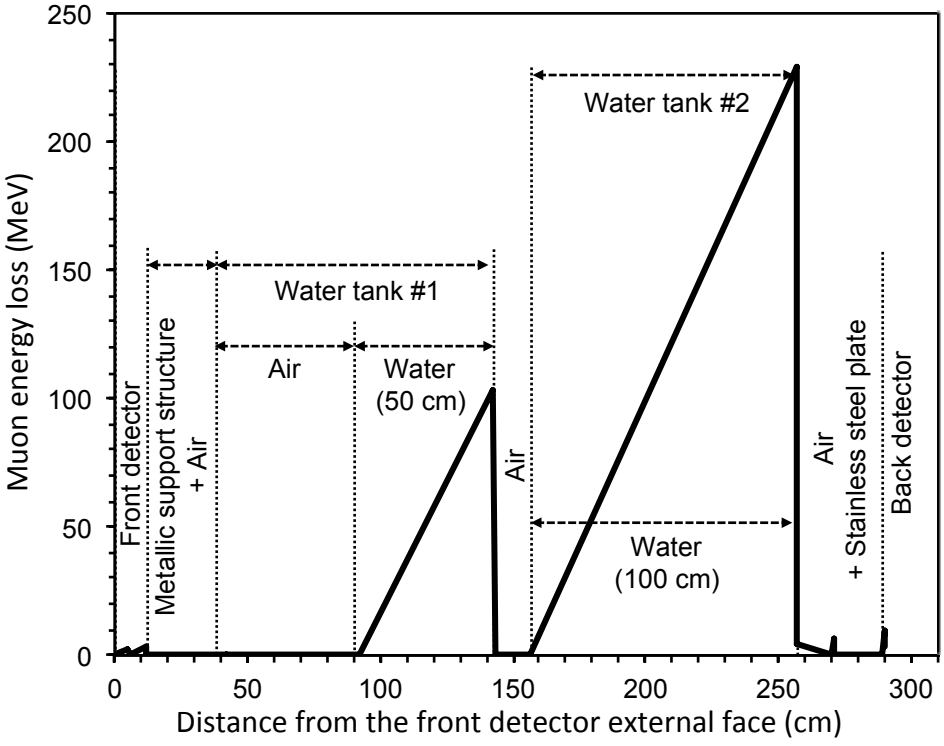

155

Figure 4. TRIM simulation showing the muon energy loss through the water tank spectrometer for an incident energy of 374 MeV. The water height is 50 cm in the first water tank and 100 cm in the second tank.

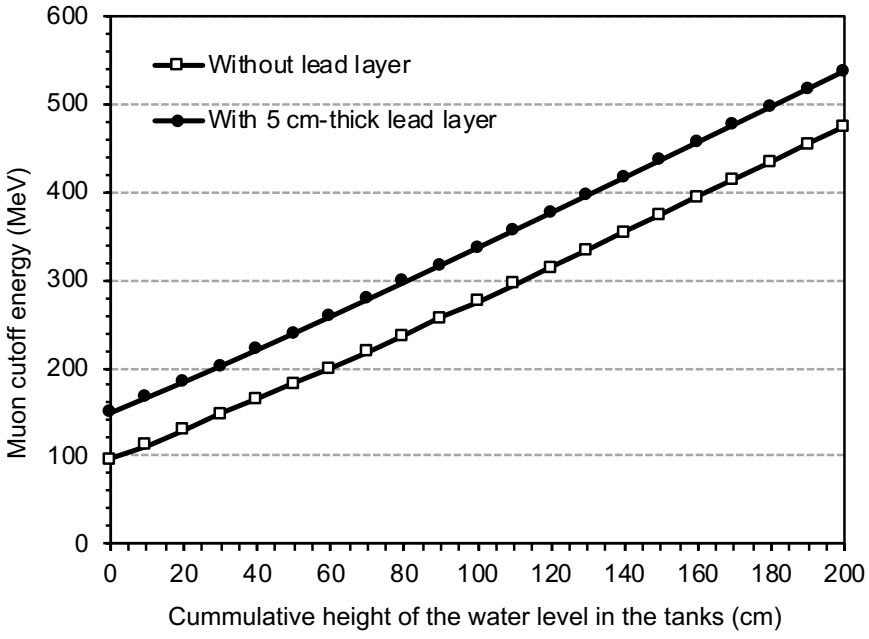

Figure 5. Muon cutoff energy of the spectrometer as a function of the cumulative height of the water level in the two water tanks with and without the optional 50 mm-thick lead layer.

2.3.2. Modeling of the spectrometer counting rate

The spectrometer counting-rate has been numerically estimated from a model directly derived from the work of Sullivan [24] and Thomas and Willis [25]. Figure 6 introduces the notations used in the following. For an anisotropic distribution of incident muons I ($m^{-2}s^{-1}sr^{-1}$) following a power cosine law with the zenithal angle θ:

$$I = I_0 cos^n(\theta) \quad (1),$$

the counting rate CR (s^{-1}) of the spectrometer fixedly pointing in the vertical direction can be easily expressed as [25]:

$$\mathrm{CR} = I_0 \eta_F \eta_B \int_{-L}^{L}\int_{-L}^{L}\int_{-L}^{L}\int_{-L}^{L} \frac{Z^{n+2}}{[Z^2+(x_2-x_1)^2+(y_2-y_1)^2]^{n+1}}\, dx_1\, dx_2 dy_1 dy_2 \qquad (2)$$

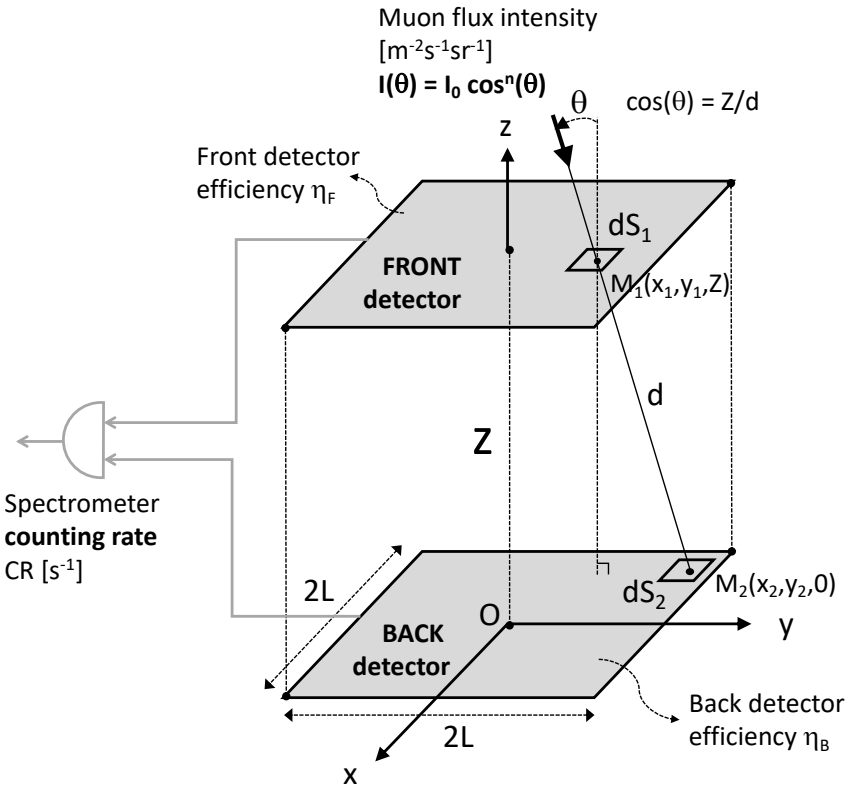

Figure 6. Schematics of the front and back detectors, and definition of axes, angles and different quantities used in the modeling of the spectrometer counting rate. For the setup shown in Fig. 1, main dimensions are Z = 2.815 m and L = 0.25 m.

where I_0 is the vertical muon flux (expressed in m^{-2} s^{-1} sr^{-1}) integrated over the energy range of the instrument, η_F and η_B are the front and back detector efficiencies, respectively, and Z is the distance between the two square detectors of surface $4L^2$ (see Figure 6).

Assuming that the zenith angle distribution of muons follows Eq. (1) with a fixed value of exponent n in the energy range of interest of the instrument, Eq. (2) directly gives the value of I_0 for each experimental counting rate CR corresponding to a given water height in the tank, i.e. to a given cutoff energy E_{min}.

For n = 2, Eq. (2) can be expressed analytically and the counting rate of the instrument is then given by:

$$CR_{n=2}^{a} = I_0 \eta_F \eta_B \times 2L \left[\frac{Z^2+8L^2}{\sqrt{Z^2+4L^2}} \times arctan\left(\frac{2L}{\sqrt{Z^2+4L^2}}\right) - Z \times arctan\left(\frac{2L}{Z}\right) \right] \quad (3)$$

where the superscript "a" is for "analytical" and the subscript "n=2" indicates that this expression is restricted to this particular value of parameter n.

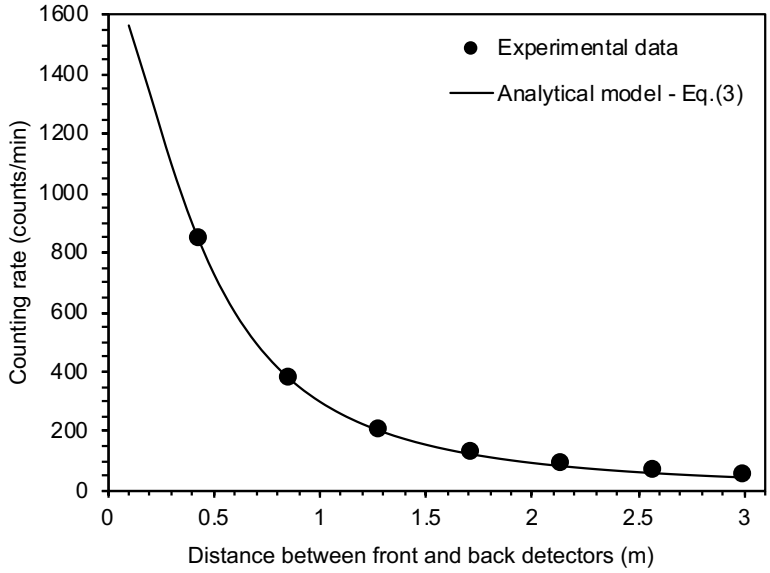

Figure 7. Counting rate as a function of the distance between the front and back detectors. The experimental data are obtained using an additional setup based on a plastic shelf described in [19]. The curve labeled "Model" is obtained from Eq. (3) with I_0 = 100 μ $m^{-2}.s^{-1}.sr^{-1}$ and n = 2.0, as experimentally obtained in [19].

3. Experimental results: sea level measurements

The muon spectrometer has been assembled indoors, on the ground floor of the experimental hall of a steel-frame industrial building with a single floor (concrete slab, thickness 10 cm) and a metal roof. The building is located on the Aix-Marseille University campus of Saint-Jérôme (Marseille, France, +43.337732°N, +5.412108°E, altitude 118 m).

198 To check the validity of the spectrometer counting-rate modeling (Eq. 3), we performed
199 preliminary measurements by varying the distance Z between the two detectors, using a
200 plastic resin shelf with seven regularly spaced shelves. In this case, the two detectors were
201 temporarily removed from the spectrometer setup and aligned vertically on two shelves of this
202 complementary characterization setup. Figure 7 shows the results of the model
203 characterization: the experimental data are in very good agreement in a distance range
204 between 40 cm and 3 m with the results of simulation using the analytical model (Eq. (3))
205 presented above, taking values $I_0 = 100\ \mu\ m^{-2}.s^{-1}.sr^{-1}$ and n = 2.0, as experimentally obtained
206 in [19].

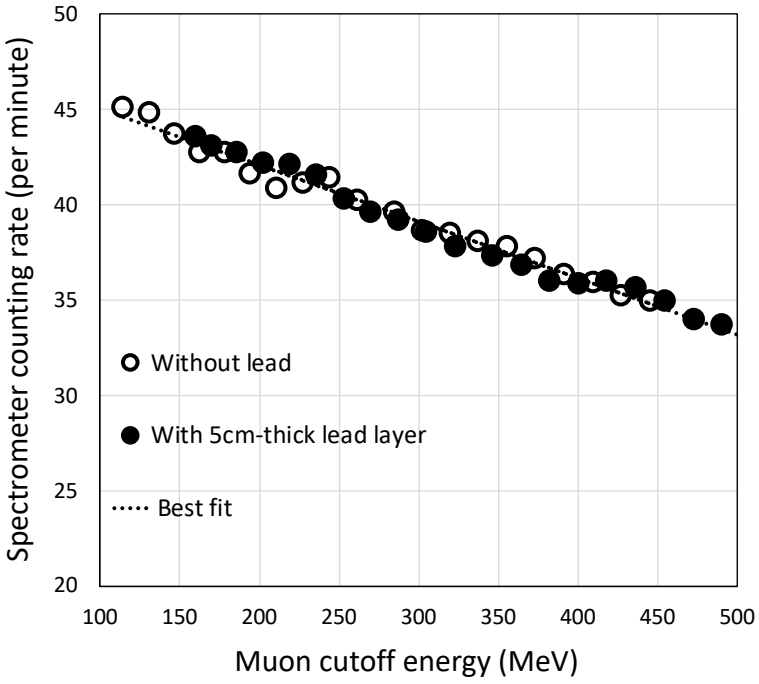

207

208 **Figure 8.** Experimental counting rates (with and without the 50 mm-tick lead layer) as a
209 function of the cutoff energy of the spectrometer. Each point corresponds to a value averaged
210 over one week (168 h).

211 After this preliminary step, the muon spectrometer was continuously operated for around
212 nine months for the acquisition of experimental data. Figure 8 shows the variations of the
213 instrument counting rate as a function of the energy cutoff E_{min} determined by the height of

214 the water level in the water tanks. Two series of data have been acquired, with and without
215 the 50 mm-thick lead layer. Each point corresponds to a value averaged over one week (168
216 hours). These results show a quasi-linear decreasing relationship between the counting rate
217 and the instrument cutoff energy. They also show that the presence of the additional lead layer
218 in the instrument material stack does not alter this linear dependency and only shift by ~50
219 MeV the energy domain explored by the instrument.

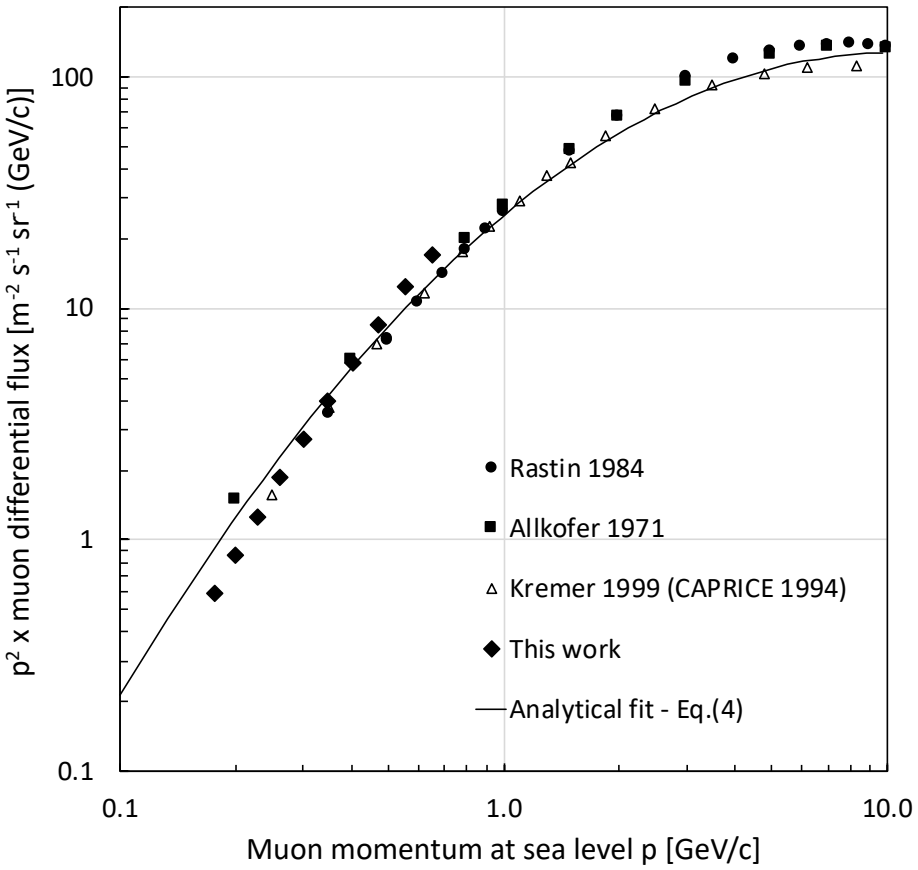

220

221 **Figure 9.** Muon spectrum at sea level deduced from data of Figure 8 and measured in other
222 experiments [3,4,5]. The line refers to the fit of experimental data with Eq. (4) and data
223 parameter from [26]. The fluxes are multiplied by p^2, where p is the momentum in GeV/c.

224 From data of Figure 8 and considering the analytical equation (3), the integral vertical
225 muon flux I_0 above energy E_{min} can be extracted from the experimental counting rate value
226 for each value of E_{min} varying from ~100 to ~500 MeV (for a muon rest mass of 105.659

MeV, the corresponding muon momentum ranges from 0.176 to 0.596 GeV/c). Considering the first derivative of this $I_0(E_{min})$ relationship (using the best linear fit on three consecutive points delimiting a small energy interval), we deduced the muon differential flux values reported in Figure 9. Experimental data measured in other published works [3,4,5] are also shown for comparison. Our values ideally complete the muon spectrum in an energy domain where only a few and sparse data were previously reported, especially below 200 MeV. These data are also consistent with previously published data and fits, in particular with the parabola-fitting model on a log-log scale given by [26]:

$$\log \mathrm{I}(\theta) = \mathrm{a}\, ln^2\, p + b\, ln\, p + c \qquad (4)$$

where p is the muon momentum in GeV/c and a, b, and c are three fitting parameters.

The analytical fit shown in Figure 9 has been obtained with Eq. (4) considering the values of a, b, and c reported in [26] for a vertical zenith angle: a = -0.1292, b = -0.266 and c = -2.600. We observe that our data satisfactory agree with this analytical fit in the full energy domain covered by the instrument.

4. Conclusion

In this work, we developed an original setup, called "water tank muon spectrometer", to measure the energy distribution of low energy atmospheric muon in the energy range 100 to 500 MeV (momentum range 0.176 to 0.596 GeV/c) not yet covered by other ground-level instruments. The instrument use water as muon moderator and a controllable water height up to 2m to vary the muon cutoff energy. The differential flux for vertical muons at sea level (43°N of latitude) has been deduced from experimental measurements combined with the numerical modeling of the instrument. Differential flux values obtained between 100 and 500 MeV are consistent with previously published data and parabola fitting model available in literature. A short-term development will automate the filling and emptying of the water tanks,

in order to make the measurements fully controllable by computer. With such an automated instrument, middle-term work will consist in a continuous muon flux monitoring to evidence possible flux variations as a function of various environment parameters.

Acknowledgments

This work has been conjointly supported by France's General Directorates DGA and DGE, under convention #132906128 (EVEREST project). The authors would like to thank T. Saad Saoud, A. Bchini, F. Derivaux and J. Beranger for their technical assistance during the development of the spectrometer.

References

[1] S. Cecchini, M. Spurio, Atmospheric muons: Experimental aspects, Geosci. Instrum. Methods Data Syst. 1 (2012) 185–196.

[2] P.K.F. Grieder, Cosmic Rays at Earth, Elsevier Press, Netherlands, 2001.

[3] O.C. Allkofer, H. Jokisch, A survey on the recent measurements of the absolute vertical cosmic-ray muon flux at sea level, Nuovo Cim. A15 (1973) 371-389.

[4] B.C. Rastin, An accurate measurement of the sea-level muon spectrum within the range 4 to 3000 GeV/c, J. Phys. G: Nucl. Phys. (1984) 10 1609.

[5] J. Kremer, M. Boezio, M. L. Ambriola, G. Barbiellini, S. Bartalucci, R. Bellotti, D. Bergström, U. Bravar, F. Cafagna, P. Carlson, M. Casolino, M. Castellano, F. Ciacio, M. Circella, C. De Marzo, M. P. De Pascale, T. Francke, N. Finetti, R. L. Golden, C. Grimani, M. Hof, W. Menn, J. W. Mitchell, A. Morselli, J. F. Ormes, P. Papini, S. Piccardi, P. Picozza, M. Ricci, P. Schiavon, M. Simon, R. Sparvoli, P. Spillantini, S. A. Stephens, S. J. Stochaj, R. E. Streitmatter, M. Suffert, A. Vacchi, N. Weber,N. Zampa, Measurements of Ground-Level Muons at Two Geomagnetic Locations, Phys. Rev. Lett. (1999) 83, 4241.

[6] V.A. Naumov, Atmospheric muons and neutrinos. Proceedings of the 2nd Workshop on Methodical Aspects of Underwater/Ice Neutrino Telescopes, Hamburg, Germany, (2001), 31-46.

[7] T. Gaisser, R. Engel, E. Resconi, Atmospheric muons and neutrinos. In Cosmic Rays and Particle Physics (2016), pp. 126-148. Cambridge: Cambridge University Press.

[8] J.L. Autran, D. Munteanu, Soft Errors: From Particles to Circuits, Taylor & Francis/CRC Press, 2015, p. 439.

[9] D. Munteanu and J.L. Autran, Modeling and Simulation of Single-Event Effects in Digital Devices and ICs, IEEE Trans. Nucl. Sci., vol. 55, no. 4, pp. 1854-1878, 2008.

[10] J.L. Autran, D. Munteanu, P. Roche, G. Gasiot, S. Martinie, S. Uznanski, S. Sauze, S. Semikh, E. Yakushev, S. Rozov, P. Loaiza, G. Warot, M. Zampaolo, Soft-errors induced by terrestrial neutrons and natural alpha-particle emitters in advanced memory circuits at ground level, Microelectron. Reliab. 50 (2010) 1822–1831.

[11] J.L. Leray, Effects of atmospheric neutrons on devices, at sea level and in avionics embedded systems, Microelectron. Reliab. 47 (2007) 1827–1835.

[12] J.L. Autran, S. Serre, D. Munteanu, S. Martinie, S. Sauze, S. Uznanski, G. Gasiot, P. Roche, Real-time soft-error testing of 40 nm SRAMs, in: 2012 Proceeding of the IEEE International Reliability Physics Symposium, IRPS, 2012, pp. 3C.5.1–3C.5.9.

[13] S. Semikh, S. Serre, J.L. Autran, D. Munteanu, S. Sauze, E. Yakushev, S. Rozov, The plateau de bure neutron monitor: Design, operation and Monte-Carlo simulation, IEEE Trans. Nucl. Sci. 59 (2) (2012) 303–313.

[14] J.L. Autran, D. Munteanu, P. Roche, G. Gasiot, Real-time soft-error rate measurements: A review, Microelectron. Reliab. 54 (2014) 1455–1476.

[15] B.D. Sierawski, M.H. Mendenhall, R.A. Reed, M.A. Clemens, R.A. Weller, R.D. Schrimpf, E.W. Blackmore, M. Trinczek, B. Hitti, J.A. Pellish, R.C. Baumann, S.- J. Wen, R. Wong, N. Tam, Muon-induced single event upsets in deep-submicron technology, IEEE Trans. Nucl. Sci. 57 (6) (2010) 3273–3278.

[16] B.D. Sierawski, R.A. Reed, M.H. Mendenhall, R.A. Weller, R.D. Schrimpf, S.-J. Wen, R. Wong, N. Tam, R.C. Baumann, Effects of scaling on muon-induced soft errors, in: 2011 Proceeding of the IEEE International Reliability Physics Symposium, IRPS, 2011.

[17] S. Serre, S. Semikh, J.L. Autran, D. Munteanu, G. Gasiot, P. Roche, Effects of Low Energy Muons on Electronics: Physical Insights and Geant4 Simulation, Proc. 13th Eur.

Conf. Radiation and its Effects on Components and Systems (RADECS), Biarritz, France, Sept. 2012. Available online : http://ms151u12.im2np.fr/news/articles/RADECS2012_Muons_Proceedings.pdf

[18] P. Roche, J.L. Autran, G. Gasiot, D. Munteanu, Technology downscaling worsening radiation effects in bulk: SOI to the rescue, in: IEEE International Electron Device Meeting, IEDM, 2013, pp. 766–769.

[19] J.L. Autran, D. Munteanu, T. Saad Saoud, S. Moindjie, Characterization of Atmospheric Muons at Sea Level Using a Cosmic Ray Telescope, Nuclear Instruments and Methods in Physics Research A, 903 (2018) 77-84.

[20] http://www.eljentechnology.com/index.php/component/content/article/31-general/48-ej-200

[21] D.E. Groom, et al., At. Data Nucl. Data Tables 78 (2001) 183–356.

[22] J.F. Ziegler, J.P. Biersack, U. Littmark, The Stopping and Range of Ions in Matter, Pergamon, New York, 1985.

[23] H.H.K. Tang, SEMM-2: A new generation of single-event-effect modeling tools, IBM J. Res. Dev. 52 (2008) 233–244.

[24] J.D. Sullivan, Geometrical factor and directional response of single and multi-element particle telescopes, Nucl. Instrum. Methods 95 (1971) 5–11.

[25] G.R. Thomas, D.M. Willis, Analytical derivation of the geometric factor of a particle detector having circular or rectangular geometry, J. Phys. E 5 (3) (1971) 261–263.

[26] J. Kempa, A. Krawczynska, Low energy muons in the cosmic radiation, Nuclear Physics B (Proc. Suppl.) 151 (2006) 299–302.